



Five mutations in N-terminus confer thermostability on mesophilic xylanase

Shan Zhang^a, Kai Zhang^b, Xiuzhen Chen^a, Xin Chu^a, Fei Sun^b, Zhiyang Dong^{a,*}

^a State Key Laboratory of Microbial Resources, Institute of Microbiology, Chinese Academy of Sciences, Beijing 100101, PR China

^b National Laboratory of Biomacromolecules, Institute of Biophysics, Chinese Academy of Sciences, Beijing 100101, PR China

ARTICLE INFO

Article history:

Received 9 March 2010

Available online 31 March 2010

Keywords:

Xylanase
Thermostability
N-terminus
Chimera
Mutant

ABSTRACT

The termini of a pair of xylanases, one of mesophilic and one of thermophilic origin, was studied by molecular dissection and systematic mutagenesis. The thermostability of the mesophilic xylanase SoxB from *Streptomyces olivaceovirdis* was significantly improved by substituting its 33 N-terminal amino acid residues with the corresponding residues of the thermophilic xylanase TfxA from *Thermomonospora fusca*. Five amino acid substitutions, which clustered in one of the regions of the N-terminus, were discovered, for the first time, to account for the majority of the improvement in thermostability of SoxB. Further systematic mutagenesis and analysis of the five mutations demonstrated that comprehensive synergism of the five mutations was involved in conferring the thermostability on the SoxB. Moreover, when the five thermostabilizing mutations were introduced into two other G/11 xylanases, SlxB from *Streptomyces lividans* and AnxB from *Aspergillus niger*, their thermostabilities were also dramatically enhanced.

© 2010 Elsevier Inc. All rights reserved.

1. Introduction

Endo-1,4- β -xylanases (EC 3.2.1.8) hydrolyze the β -1,4-glycosidic bonds of β -1,4-xylan, the major plant cell wall polysaccharide component of hemicellulose [1]. On the basis of primary sequence homology and hydrophobic cluster analysis, the xylanases have been grouped into two families (family F/10 and family G/11) [2]. The overall structure of the G/11 xylanase catalytic domain folds into two β -sheets and one short α -helix and resembles a partly closed right hand [3]. The importance of the N-termini, which are situated at the edge of the β -sheets, in maintaining the thermostability of G/11 xylanases, was highlighted by a large number of research endeavors to improve the thermostability of G/11 xylanases [4–10].

TfxA from the filamentous soil thermophile *Thermomonospora fusca* is known to be one of the most thermostable G/11 xylanases [11,12]. It has been assumed that N-terminus replacement with the corresponding segment from thermophilic xylanase TfxA could be an efficient technique to improve the thermostability of mesophilic xylanase [12]. However, little detailed work on the N-terminus has been carried out. Therefore, an obvious but important question remains poorly explained: why could the substitution of the N-terminus of TfxA improve the thermostability of the mesophilic xylanase homolog?

Streptomyces olivaceovirdis XynB SoxB [13] is one of the mesophilic G/11 xylanases that shares the greatest amino acid sequence identity (74%) with that of the catalytic domain of the thermophilic TfxA. However, the sequence identity of the 33 N-terminal residues (numbered by the SoxB sequence) between SoxB and TfxA is as low as 48%. This, to some extent, has underscored the importance of the N-termini of G/11 xylanases for their thermostabilities. A chimeric xylanase, STxAB, was generated by substituting the N-terminus of TfxA for the corresponding region of the *S. olivaceovirdis* xylanase SoxB. This chimera and the wild type SoxB, which share the same sequence except the N-terminus, provided a pair of desirable xylanases for comprehensive investigation of the potential thermostabilizing effect of the N-terminus of TfxA.

2. Materials and methods

2.1. Construction and overproduction of wild types, chimera and mutant xylanases

The xylanase genes SoxB, TfxA, SlxB and AnxB were cloned from *S. olivaceovirdis* ATCC 23630 strain, *T. fusca* ATCC 27730 strain, *Streptomyces lividans* ATCC 19844 strain and *Aspergillus niger* UV-11, respectively, by the PCR method. All the genes of the chimera and mutant xylanases were constructed by overlap extension PCR [14]. All mutations were confirmed by sequencing of the entire xylanase genes. All of the xylanase genes were digested with NdeI and EcoRI and ligated into pET-28a (+), then expressed in *Escherichia coli* BL21 (DE3) cells. For the wild types and all the chimera and mutant xylanases, a single-step cation exchange purification protocol yielded pure protein as evaluated by

* Corresponding author. Address: State Key Laboratory of Microbial Resources, Institute of Microbiology, Chinese Academy of Sciences, Datun Road, Chaoyang District, Beijing 100101, PR China. Fax: +86 10 6480 7337.

E-mail address: dongzy@sun.im.ac.cn (Z. Dong).

Coomassie-stained SDS-PAGE [15]. Protein concentration was determined by the BCA method using bovine serum albumin (BSA) as the protein standard.

2.2. Enzyme activity assay

Endo-1, 4- β -xylanase (EC 3.2.1.8) activity was measured by the dinitrosalicylic acid (DNS) method [16]. Briefly, 40 μ l of diluted enzyme were mixed with 360 μ l of a 10 mg/ml suspension of birchwood xylan (Sigma–Aldrich) and incubated for 10 min at 50 °C. Then 600 μ l of DNS reagent were mixed and incubated for 15 min at 99 °C. One international unit (IU) is defined as the amount of enzyme that releases 1 μ mol of reducing sugar per minute.

2.3. Thermal inactivation and optimum catalytic temperature

Half-lives of thermal inactivation of the wild type and mutant xylanases were determined by heat challenge in the absence of substrate in 50 mM sodium acetate buffer (pH 6.0). At various time intervals, 40 μ l aliquots were removed and the residual activity was measured as described above. The half-life curves were fitted to equation $y = A e^{-kt}$ by the Excel Microsoft Program [5]. The optimum catalytic temperature was measured in 50 mM sodium acetate buffer (pH 6.0) at various temperatures in the presence of substrate.

2.4. Determination of melting temperature by differential scanning calorimetry (DSC)

DSC experiments were performed using a Nano DSC (TA Instruments) with sample concentrations of 1 mg/ml at a scan rate of 1 °C/min. A constant pressure of 3 atm was maintained during all DSC experiments to prevent possible degassing of the solution upon heating. Reversibility of the thermally induced transitions was determined by reheating the sample in the calorimeter cell immediately after cooling the first run. The DSCRun software package was used for data acquisition. CpConvert was used for the conversion from microwatts into molar heat capacity. Due to the irreversibility of the denaturation in the wild type and mutant xylanases, only apparent melting temperatures (T_m) could be calculated and compared [17,18]. Baseline subtracted DSC data were normalized for protein concentration and used to determine the T_m value.

2.5. Homology modeling, optimization and structure analysis

Two of the homologous crystal structures (PDB codes: 1HIX and 1M4W) with the highest sequence identity and lowest number of insertions and deletions were chosen as the templates. The software package modeler [19,20] was used for modeling SoxB from the two templates, which involved the calculation of distance

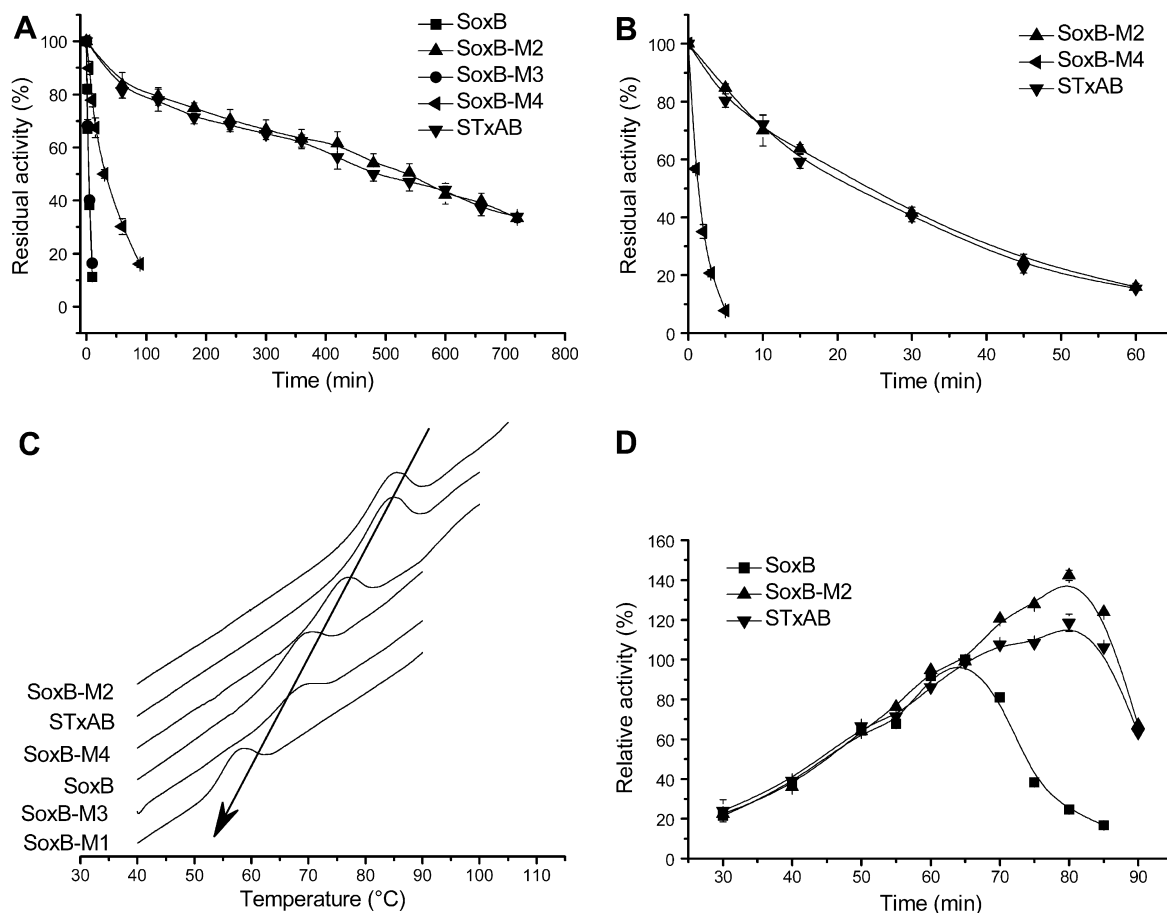


Fig. 1. The thermostabilities of wild type SoxB and mutant xylanases. Thermal inactivation profiles were determined at 70 °C (A) or 80 °C (B) for the purified wild type SoxB, four regional mutants (SoxB-M1, SoxB-M2, SoxB-M3 and SoxB-M4) and the chimeric xylanase STxAB. (C) The apparent T_m values were determined by DSC for the regional mutants and wild type xylanase. The microwatts from the DSC were converted into the corresponding molar heat capacity (C_p). The C_p values were then normalized and used to produce the waterfall plot for SoxB and regional mutants. The apparent T_m values of regional mutants and wild type xylanase were arranged in descending order. (D) Temperature dependence of the activity of wild type and mutant xylanases. Relative activity (%) is characterized by P/P_{max} , where P is the amount of product at the desired temperature and P_{max} is the amount of product generated by SoxB when incubated at the optimum temperature for 10 min at pH 6.0 with 10 mg/ml birchwood xylan as the substrate.

and dihedral angle restraints from the structure-based alignment, the determination of the objective function by the combination of spatial restraints and CHARMM energy and optimization of the objective function in Cartesian space. Further refinement was performed using the program Refmac5 [21] to idealize the geometry for bond angle and bond length. The structure visualization was performed with the Coot [22] and Pymol [23] software.

3. Results

3.1. Improvement of the thermostability of the chimeric xylanase STxAB

The chimeric xylanase STxAB was produced by replacing all 33 residues of the N-terminus of SoxB with the corresponding 31 residues of the N-terminus of TfxA. The half-life at 70 or 80 °C and apparent T_m value of STxAB were analyzed and compared with that of the SoxB (Fig. 1 and Table 1). A significant increase in the thermostability of STxAB was observed and highlighted the importance of the N-terminus of TfxA in conferring the remarkably high thermostability on SoxB. In addition to improving thermostability, the chimeric xylanase STxAB also displayed an increased thermophilicity. STxAB had an optimum temperature of 80 °C, which was 15 °C higher than that of SoxB (65 °C) (Fig. 1D and Table 2). In summary, the thermostability and thermophilicity of SoxB were significantly enhanced by substituting 33 N-terminal amino acid residues of SoxB with the corresponding 31 residues of TfxA. The mechanism for the significant difference in thermostability between SoxB and STxAB was completely contained in the 33 residues of the N-termini (Fig. 2A).

3.2. Molecular dissection of the N-terminus and identification of the thermostabilizing region

As shown in Fig. 2, the divergent residue positions in the N-termini of SoxB and TfxA were grouped into four regions (R1, R2, R3 and R4) according to sequence alignment and structure analysis. Region 1 (R1) is the loop region before β -strand B1, Region 2 (R2) forms the region between β -strands B1 and B2, Region 3 (R3) is

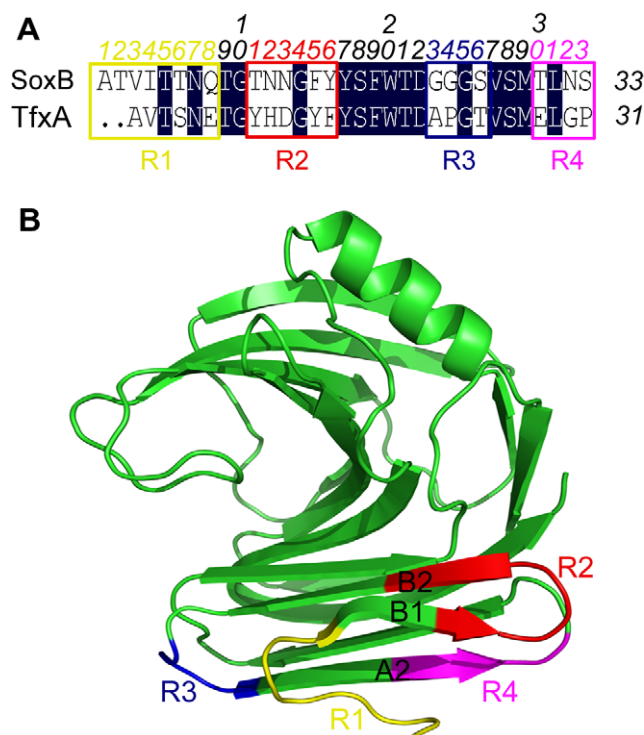


Fig. 2. Sequence alignment of the N-termini of SoxB and TfxA and the locations of Region 1–Region 4 in the overall structure of SoxB. (A) The N-termini of both xylanases were divided into four regions (R1, R2, R3 and R4), which were noted with frames in the amino acid sequence. (B) These four regions were shown in the overall structure of SoxB. R1 (in yellow) is the loop region before β -strand B1; R2 (in red) forms the region between β -strands B1 and B2; R3 (in blue) is the loop region between β -strands B2 and A2; R4 (in magenta) is situated in the C-terminal region of β -strand A2. (For interpretation of the references to color in this figure legend, the reader is referred to the web version of this article.)

the loop region between β -strand B2 and β -strand A2 and Region 4 (R4) is situated in the C-terminal region of β -strand A2 (Fig. 2B). Accordingly, four regional mutants (SoxB-M1, SoxB-M2, SoxB-M3 and SoxB-M4) of SoxB were produced by substituting

Table 1

Comparison of the thermostabilities of wild type SoxB and regional mutants.

Regions	Xylanases	Mutations	$t_{1/2}$ at 70 °C (min)	$t_{1/2}$ at 80 °C (min)	T_m (°C)	ΔT_m
N-terminus	SoxB	–	3.6	^a	69.1	–
	STxAB	N-terminus replacement	493	21	83.9	14.8
R1	SoxB-M1	A1-, T2-, V3A, I4V, T6S, Q8E	^a	^a	57.6	–11.5
R2	SoxB-M2	T11Y, N12H, N13D, F15Y, 16F	509	23	84.5	15.4
R3	SoxB-M3	G23A, G24P, S26T	3.8	^a	68.4	–0.7
R4	SoxB-M4	T30E, N32G, S33P	33	1.3	75.8	6.7

^a The xylanase lost all of its enzyme activity within only 1 min so that the $t_{1/2}$ could not be determined.

Table 2

Comparison of the thermostabilities and thermophilicities of wild types (SoxB, SlxB and AnxB) and the corresponding mutants (SoxB-M2, SlxB-M2 and AnxB-M2).

Xylanases	$t_{1/2}$ (min)	T_m (°C)	Optimum temperature (°C)	V_{max} at the optimum temperature (IU/mg)
SoxB	3.6 ^a (70 °C)	69.1	65	801 ± 22
STxAB	493 ^a (70 °C)	83.9	80	949 ± 35
SoxB-M2	509 ^a (70 °C)	84.5	80	1140 ± 21
SlxB	2.1 ^b (65 °C)	61.5	55	427 ± 18
SlxB-M2	74 ^b (65 °C)	75.7	65	462 ± 29
AnxB	12 ^c (55 °C)	54.1	50	1342 ± 61
AnxB-M2	76 ^c (55 °C)	63.2	55	1590 ± 68

^a The half-lives of SoxB, STxAB and SoxB-M2 were determined at 70 °C.

^b The half-lives of SlxB and SlxB-M2 were determined at 65 °C.

^c The half-lives of AnxB and AnxB-M2 were obtained at 55 °C.

the amino acid residues of SoxB in the four individual regions with the corresponding regions of residues in TfxA. Their half-lives and apparent T_m values were then analyzed in comparison with those of SoxB and STxAB (Fig. 1 and Table 1). SoxB-M1 decreased its thermostability significantly when compared with the wild type xylanase SoxB (Table 1). SoxB-M3 had a similar half-life to SoxB (Fig. 1A and Table 1) and its T_m value was slightly lower than that of SoxB (Fig. 1C and Table 1). Interestingly, the half-lives at 70 °C of SoxB-M4 and SoxB-M2 were increased to 33 and 509 min, respectively. It is especially worth noting that SoxB-M2, a derivative of SoxB that contains only five substituted residues in Region 2, displayed a significantly higher thermostability than SoxB and even slightly higher than STxAB (Fig. 1 and Table 1). At 70 °C, SoxB-M2 was up to 140-fold more stable than SoxB (Table 1). Furthermore, the half-lives of SoxB-M2 at 70 and 80 °C were 16 and 2 min higher than those of STxAB, respectively (Table 1). The apparent T_m value of SoxB-M2 (84.5 °C) was 15.4 and 0.6 °C higher than that of SoxB and STxAB, respectively (Fig. 1C and Table 1). Meanwhile, SoxB-M2 displayed an optimum temperature of 80 °C, which is as high as the chimeric xylanase STxAB and 15 °C higher than the wild type SoxB (Fig. 1D). The specific activity of the mutant SoxB-M2 at optimum temperature was 1.4- and 1.2-fold higher than that of wild type SoxB and the chimeric xylanase STxAB, respectively, suggesting that the mutations in SoxB-M2 did not compromise, but improved the enzyme activity (Table 2).

Thus, it seemed that the increased thermostability of STxAB is not the sum of small increments. Rather, five amino acid substitutions (T11Y, N12H, N13D, F15Y and Y16F), which clustered in the Region 2 of the N-terminus, were discovered to account for the chief difference in thermostability between the chimeric xylanase STxAB and SoxB.

3.3. Five mutations in combination confer thermostability on SoxB

Focusing on the five divergent amino acid residue positions in Region 2, the systematic mutagenesis was employed to identify the specific amino acid residue(s) involved in contributing to the thermostability of SoxB-M2. Five mutants of SoxB (SoxB-T11Y, SoxB-N12H, SoxB-N13D, SoxB-F15Y and SoxB-Y16F), each containing a single amino acid substitution at every divergent position in Region 2, were generated and analyzed for their thermostabilities. Both the thermal inactivation and DSC experiment demonstrated that the individual mutations T11Y, N12H or Y16F, had a positive but limited effect on the thermostability of SoxB, while F15Y had a negligible effect and N13D had a negative effect on the thermostability of SoxB (Table 3).

On the other hand, to test whether the five mutations in R2 were essential for SoxB-M2 thermostability, five mutants derived

from SoxB-M2 (M2-Y11T, M2-H12N, M2-D13N, M2-Y15F and M2-F16Y), each containing a single reverse mutation, were generated and their thermostabilities were subsequently analyzed. The half-lives at 70 °C of all five mutants of SoxB-M2 were decreased when compared with that of SoxB-M2 (Table 3). Meanwhile, the apparent T_m values of all the five mutants were decreased to some extent, which coincided well with the results of the thermal inactivation assay (Table 3). These results indicated that the five mutations (T11Y, N12H, N13D, F15Y and Y16F) were essential for the thermostability of SoxB-M2.

In summary, the effect on thermostability of individual mutation of the five residues in Region 2 was found to be rather limited and even adverse. And the five mutations in combination were confirmed as being essential for significant improvement in the thermostability. Therefore, the comprehensive synergism of these five mutations might be involved in conferring the thermostability on SoxB.

3.4. Thermostabilization of other xylanases by the introduction of these five mutations

To test whether other xylanases could also be stabilized by the introduction of these five mutations (T11Y, N12H, N13D, F15Y and Y16F, numbered by SoxB sequence) like in the case of SoxB-M2, two additional xylanases, SlxB and AnxB, were chosen as candidates for further investigation. The xylanase SlxB was from *S. lividans*, whose catalytic domain has 84% amino acid identity with that of SoxB. The AnxB from the fungus *A. niger* displayed a lower amino acid sequence identity (62%) with SoxB and exhibited a distinct enzyme activity and optimum temperature from SoxB and SlxB (Table 2). In the corresponding Region 2 positions, both xylanases share a similar amino acid sequence with SoxB. After introducing the five mutations (T11Y, N12H, N13D, F15Y and Y16F, numbered by SoxB sequence) into the sequences of SlxB and AnxB, both the mutants, SlxB-M2 and AnxB-M2, dramatically improved their thermostabilities when compared with their corresponding wild types (Fig. 3 and Table 2). Furthermore, the optimum temperature of the SlxB-M2 and AnxB-M2 were 10 and 5 °C higher than their corresponding wild type SlxB and AnxB, respectively. And the specific activity of the mutant SlxB-M2 and AnxB-M2 at the optimum temperature were 1.1- and 1.2-fold higher than that of corresponding wild type xylanase, respectively (Table 2).

The improvement in the thermostabilities of SlxB and AnxB by the introduction of the five mutations further confirmed the thermostabilizing effect of the five mutations discovered in the N-terminus comparison and analysis of the xylanase homologs, SoxB and TfxA.

Table 3
Systematic comparison of the effect of the individual substitution in R2 on thermostability.

	Mutants	Mutation	$t_{1/2}$ at 70 °C (min)	T_m (°C)	ΔT_m
Mutants from SoxB	SoxB	–	3.6	69.1	–
	SoxB-T11Y	T11Y	15	73.9	4.8 ^a
	SoxB-N12H	N12H	16	75.5	6.4 ^a
	SoxB-N13D	N13D	2.7	67.2	–1.9 ^a
	SoxB-F15Y	F15Y	3.6	69.0	–0.1 ^a
	SoxB-Y16F	Y16F	5.4	71.1	2.0 ^a
Mutants from SoxB-M2	SoxB-M2	–	509	84.5	–
	M2-Y11T	Y11T	205	80.7	–3.8 ^b
	M2-H12N	H12N	24	75.3	–9.2 ^b
	M2-D13N	D13N	177	80.4	–4.1 ^b
	M2-Y15F	Y15F	424	84.3	–0.2 ^b
	M2-F16Y	F16Y	289	82.6	–1.9 ^b

^a The ΔT_m values given show the T_m differences between the mutants of SoxB and wild type SoxB.

^b The ΔT_m values given show the T_m differences between the mutants derived from SoxB-M2 and SoxB-M2.

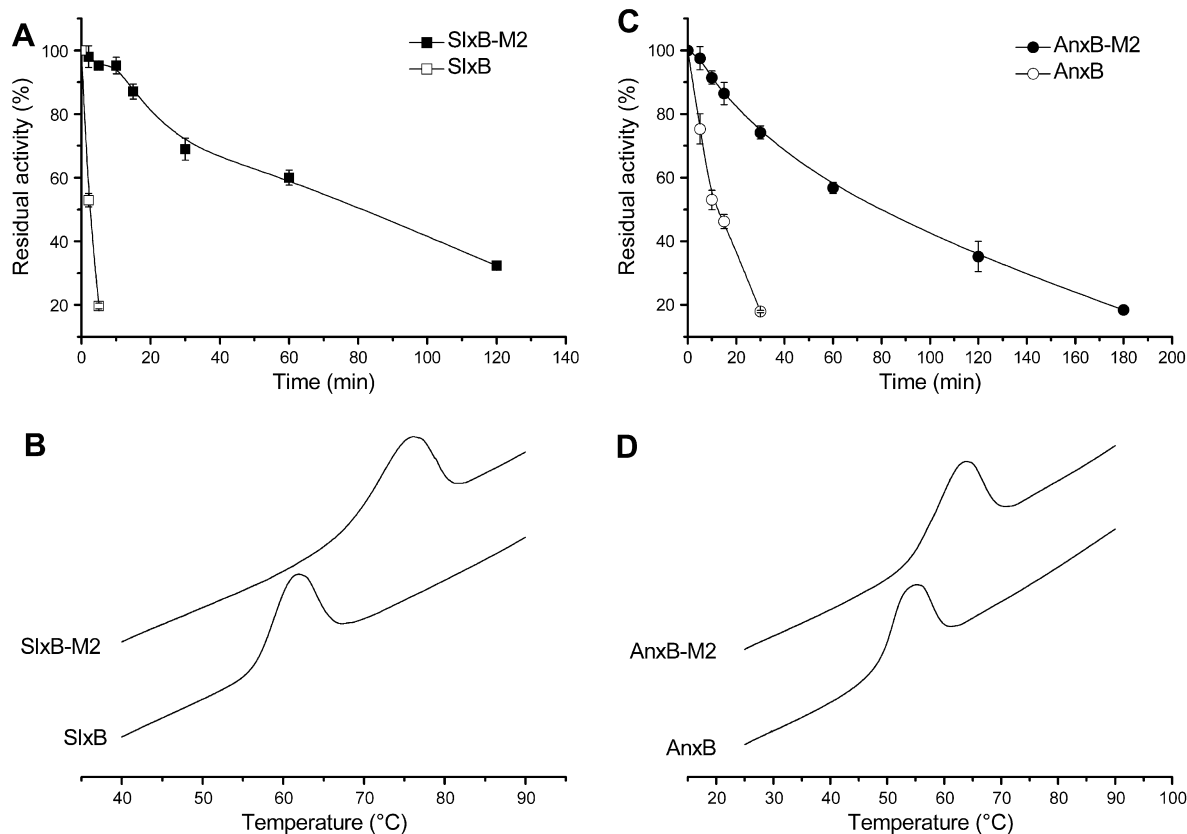


Fig. 3. Comparison of the thermostabilities of the wild type xylanases (SlxB and AnxB) and the corresponding mutant xylanases (SlxB-M2 and AnxB-M2). (A) Thermal inactivation profiles were determined at 65 °C for the purified SlxB and SlxB-M2. (B) Comparison of the apparent T_m values of the SlxB and SlxB-M2. (C) Thermal inactivation profiles were measured at 55 °C for the purified AnxB and AnxB-M2. (D) Comparison of the apparent T_m values of the AnxB and AnxB-M2. The apparent T_m values were determined by DSC. The C_p values were normalized and used to produce the waterfall plot.

4. Discussion

It had been assumed that the N-termini of the mesophilic xylanases are particularly susceptible to thermal unfolding [4]. By starting to unwind the structure from the N-terminus, one would initiate the disassembly of the whole structure and lead to cooperative unfolding of the whole protein. Here, the five mutations in Region 2 might provide additional factors for strengthening the structural stability of the N-terminus and hence prevent the thermal unfolding of the overall structure.

Two xylanases with crystal structure (PDB codes: 1HIX and 1M4W) information available shared sequence homology as high as 85% and 74% with SoxB-M2. Only the monomer form was observed for both xylanases. Also, no polymer formation was detected for SoxB-M2 and STxAB in gel filtration chromatography analyses (data not shown). Thus, the improvement in the thermostability of SoxB-M2 seemed to be the consequence of the formation of additional interactions that stabilized the local conformation.

A comparative structural analysis of SoxB-M2 and SoxB showed that the T11Y mutation in SoxB-M2 allowed for the Y11–F16 aromatic interaction, which might stabilize the local configuration between the β -strands B1 and B2 (Fig. 4) and improve the thermostability of SoxB. The SoxB-T11Y mutant, which contains a single amino acid substitution, was only 4-fold more stable at 70 °C than wild type SoxB (Table 3), which is in agreement with the research result on thermostability effect of the T11Y substitution in *Streptomyces* sp. S38 [5]. However, SoxB-M2 is 140-fold more stable than SoxB (Table 3), suggesting that the T11Y mutation accounts for only small part of the difference between the thermostabilities of SoxB-M2 and SoxB. The imidazole ring of H12 in SoxB-N12H will

make more van der Waals contacts with N13 and N32. It remains possible that N12H might produce stronger hydrogen-bond with N32 and hydrophobic interaction with L31 and Y17 (Fig. 4A). Thus, it is assumed that H12 would be more favorable than N12 for maintaining the structural stability and it is therefore another cause for the improvement in thermostability of SoxB-M2. Furthermore, the amino acid residue at the position 16 in the SoxB sequence was found in hydrophobic surrounding. It is possible that the F16 residue would be more favorable than Y16 in the hydrophobic surrounding, which might cause the slight increase in thermostability of SoxB-Y16F.

To our surprise, the single mutation N13D did not improve, but instead slightly decreased the thermostability of SoxB-N13D (Table 3). No major perturbation was found in the structure of SoxB-N13D mutant proteins relative to structure of the wild type SoxB. It is possible that the decrease in stability might be accounted for by cumulative effects of the following factors: by changes in main-chain dihedral angles and in side-chain rotomers and by the unfavorable electrostatic interactions between the D13 side chain and the carbonyls of the main chain [24]. However, by introducing the N12H and N13D mutations simultaneously, the desirable conformation formed might stabilize the regional structure due to the electrostatic interactions between H12 and D13 and the interactions around H12 and D13 residues (Fig. 4A). These results indicated the importance of cooperative interactions between H12 and D13 in maintaining the thermostability of SoxB-M2. When combined with N32 and L31 in β -strand A2, H12 and D13 in β -strand B1 or in the immediate vicinity of the connecting loop might stabilize the local configuration between the β -strands B1 and A2 and confer the thermostability on SoxB (Fig. 4A).

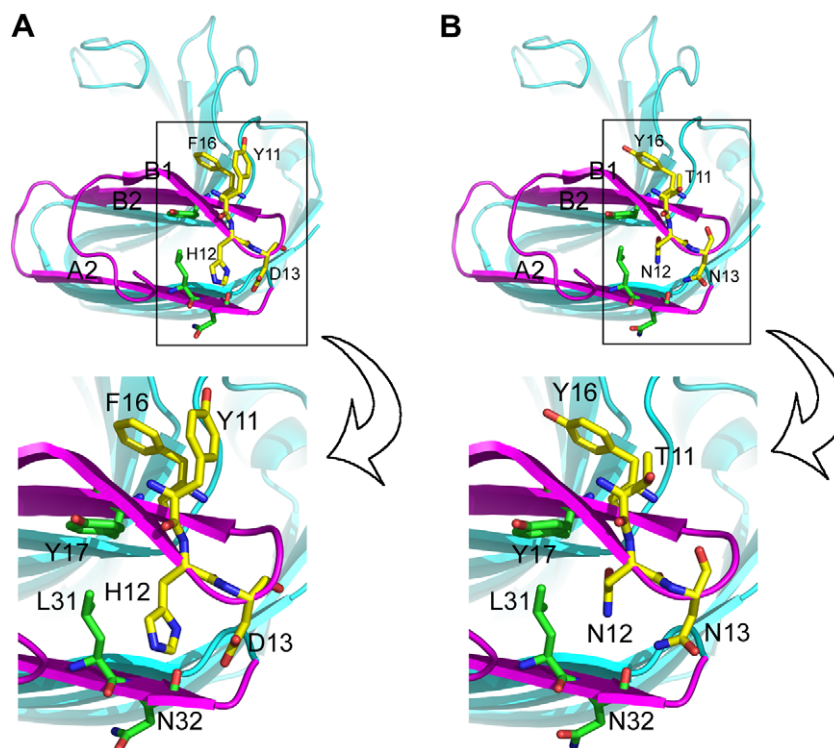


Fig. 4. Homology modeling and structure comparison of SoxB-M2 (A) and wild type SoxB (B). SoxB-M2 allowed for the more extensive hydrophobic interactions between Y11 and F16 compared with T11–Y16 in SoxB. The hydrophobic interactions between Y11 and F16 might stabilize the local configuration between the β -strands B1 and B2. The electrostatic interactions between H12 and D13 and the interactions between N32, L31, Y17 and H12 might stabilize the local configuration between the β -strands B1 and A2. Therefore, the mutations (displayed in yellow) seem to help anchor the β -strands B1, B2 and A2 in the N-terminal β -sheets and make the structure of N-terminus more thermally stable. The N-termini of both xylanases are displayed in magenta. The figure was produced using PyMOL. (For interpretation of the references to color in this figure legend, the reader is referred to the web version of this article.)

In conclusion, the thermal inactivation and DSC experiments were in agreement with each other and demonstrated that not all of the residues in the N-terminus of TfxA were involved in conferring thermostability on SoxB. Rather, the five mutations in R2 (T11Y, N12H, N13D, F15Y and Y16F) were responsible for the majority of the improvement in thermostability. The five mutations seemed to confer the thermostability on SoxB through both additive (the thermostabilizing effect of the individual mutations T11Y, N12H and Y16F) and cooperative (the H12–D13 electrostatic interaction and Y11–F16 hydrophobic interaction) effects. Y11, H12 and D13 in β -strand B1 or in the immediate vicinity of the connecting loop, F16 and Y17 in β -strand B2 and L31 and N32 in β -strand A2, which seem to help anchor the β -strands B1, B2 and A2 in the N-terminal β -sheets through the synergism, make the structure of the N-terminus more thermally stable (Fig. 4).

Moreover, the present work provided a new approach to obtain thermostable xylanases by the substitution of fewer critical residues rather than N-terminal replacement during which many more amino acid mutations are ambiguously involved in the protein engineering. The results are also encouraging when considering future attempts to introduce the five thermostabilizing residues into more potential G/11 xylanases with different features.

Acknowledgments

We thank Junjie Luo (Department of Chemistry, Tsinghua University) for technical assistance. This work was supported by Project “863” of National High Technology Research and Development Program (No. 2007AA100604 to Zhiyang Dong).

References

- [1] T. Collins, C. Gerday, G. Feller, Xylanases, xylanase families and extremophilic xylanases, *FEMS Microbiol. Rev.* 29 (2005) 3–23.
- [2] B. Henrissat, A classification of glycosyl hydrolases based on amino acid sequence similarities, *Biochem. J.* 280 (1991) 309–316.
- [3] A. Sapag, J. Wouters, C. Lambert, P. de Ioannes, J. Eyzaguirre, E. Depiereux, The endoxylanases from family 11: computer analysis of protein sequences reveals important structural and phylogenetic relationships, *J. Biotechnol.* 95 (2002) 109–131.
- [4] C. Dumon, A. Varvak, M.A. Wall, J.E. Flint, R.J. Lewis, J.H. Lakey, C. Morland, P. Luginbuhl, S. Healey, T. Todaro, Engineering hyperthermostability into a GH11 xylanase is mediated by subtle changes to protein structure, *J. Biol. Chem.* 283 (2008) 22557–22564.
- [5] J. Georis, F.D.L. Esteves, J. Lamotte-Brasseur, V. Bougnat, B. Devreese, F. Giannotta, B. Granier, J.M. Frere, An additional aromatic interaction improves the thermostability and thermophilicity of a mesophilic family 11 xylanase: structural basis and molecular study, *Protein Sci.* 9 (2000) 466–475.
- [6] N. Hakulinen, O. Turunen, J. Janis, M. Leisola, J. Rouvinen, Three-dimensional structures of thermophilic β -1,4-xylanases from *Chaetomium thermophilum* and *Nonomuraea flexuosa*: comparison of twelve xylanases in relation to their thermal stability, *Eur. J. Biochem.* 270 (2003) 1399–1412.
- [7] R. Ruller, L. Deliberto, T.L. Ferreira, R.J. Ward, Thermostable variants of the recombinant xylanase from *Bacillus subtilis* produced by directed evolution show reduced heat capacity changes, *Proteins Struct. Funct. Bioinform.* 70 (2008) 1280–1293.
- [8] W.L. Sung, J. Tolan, Thermostable xylanase, Patent US-7060482, National Research Council of Canada, Ottawa, Canada, 2006.
- [9] O. Turunen, K. Etuaho, F. Fenel, J. Vehmaanper, X. Wu, J. Rouvinen, M. Leisola, A combination of weakly stabilizing mutations with a disulfide bridge in the α -helix region of *Trichoderma reesei* Endo-1,4- β -xylanase II increases the thermal stability through synergism, *J. Biotechnol.* 88 (2001) 37–46.
- [10] W.W. Wakarchuk, W.L. Sung, R.L. Campbell, A. Cunningham, D.C. Watson, M. Yaguchi, Thermostabilization of the *Bacillus circulans* xylanase by the introduction of disulfide bonds, *Protein Eng. Des. Sel.* 7 (1994) 1379–1386.
- [11] D. Irwin, E.D. Jung, D.B. Wilson, Characterization and sequence of a *Thermomonospora fusca* xylanase, *Appl. Environ. Microbiol.* 60 (1994) 763–770.

- [12] H. Shibuya, S. Kaneko, K. Hayashi, Enhancement of the thermostability and hydrolytic activity of xylanase by random gene shuffling, *Biochem. J.* 349 (2000) 651–656.
- [13] X. Su, S. Zhang, L. Wang, Z. Dong, Overexpression of lbpB enhances production of soluble active *Streptomyces olivaceovirdis* XynB in *Escherichia coli*, *Biochem. Biophys. Res. Commun.* 390 (2009) 673–677.
- [14] R.M. Horton, H.D. Hunt, S.N. Ho, J.K. Pullen, L.R. Pease, Engineering hybrid genes without the use of restriction enzymes: gene splicing by overlap extension, *Gene* 77 (1989) 61–68.
- [15] U.K. Laemmli, Cleavage of structural proteins during the assembly of the head of bacteriophage T4, *Nature* 227 (1970) 680–685.
- [16] M.J. Bailey, P. Biely, K. Poutanen, Interlaboratory testing of methods for assay of xylanase activity, *J. Biotechnol.* 23 (1992) 257–270.
- [17] J.M. Sanchez-Ruiz, Theoretical analysis of Lumry–Eyring models in differential scanning calorimetry, *Biophys. J.* 61 (1992) 921–935.
- [18] N. Palackal, Y. Brennan, W.N. Callen, P. Dupree, G. Frey, F. Goubet, G.P. Hazlewood, S. Healey, Y.E. Kang, K.A. Kretz, An evolutionary route to xylanase process fitness, *Protein Sci.* 13 (2004) 494–503.
- [19] N. Eswar, B. Webb, M.A. Marti-Renom, M.S. Madhusudhan, D. Eramian, M.Y. Shen, U. Pieper, A. Sali, Comparative protein structure modeling using Modeller, *Curr. Protocols Protein Sci.* Chapter 2, Unit 29, 2007.
- [20] A. Sali, T.L. Blundell, Comparative protein modelling by satisfaction of spatial restraints, *J. Mol. Biol.* 234 (1993) 779–815.
- [21] Collaborative Computational Project, The CCP4 suite: programs for protein crystallography, *Acta Crystallogr. Sect. D Biol. Crystallogr.* 50 (1994) 760–763.
- [22] P. Emsley, K. Cowtan, Coot: model-building tools for molecular graphics, *Acta Crystallogr. Sect. D Biol. Crystallogr.* 60 (2004) 2126–2132.
- [23] W.L. DeLano, The PyMOL Molecular Graphics System, DeLano Scientific, San Carlos, CA, 2002.
- [24] P.R. Pokkuluri, M. Gu, X. Cai, R. Raffin, F.J. Stevens, M. Schiffer, Factors contributing to decreased protein stability when aspartic acid residues are in β -sheet regions, *Protein Sci.* 11 (2002) 1687–1694.